Homogeneous crystallization in cyclically sheared frictionless grains

Weiwei Jin*,[1] Corey S. O'Hern,[1, 2, 3] Charles Radin,[4] Mark D. Shattuck**,[5] and Harry L. Swinney[6]

[1]*Department of Mechanical Engineering and Materials Science,*
Yale University, New Haven, Connecticut 06520, USA
[2]*Department of Physics, Yale University, New Haven, Connecticut 06520, USA*
[3]*Department of Applied Physics, Yale University, New Haven, Connecticut 06520, USA*
[4]*Department of Mathematics, University of Texas at Austin, Austin, Texas 78712, USA*
[5]*Benjamin Levich Institute and Physics Department,*
The City College of New York, New York, New York 10031, USA
[6]*Center for Nonlinear Dynamics and Department of Physics,*
University of Texas at Austin, Austin, Texas 78712, USA

Many experiments over the past half century have shown that, for a range of protocols, granular materials compact under pressure and repeated small disturbances. A recent experiment on cyclically sheared spherical grains showed significant compaction via homogeneous crystallization (Rietz *et al.*, 2018). Here we present numerical simulations of frictionless, purely repulsive spheres undergoing cyclic simple shear with dissipative Newtonian dynamics at fixed vertical load. We show that for sufficiently small strain amplitudes, cyclic shear gives rise to homogeneous crystallization at a volume fraction $\phi = 0.646 \pm 0.001$. This result indicates that neither friction nor gravity is essential for homogeneous crystallization in driven granular media.

Loose granular materials will compact under a range of different protocols of small repeated disturbances while under the influence of gravity and/or external pressure. In the half century following the pioneering work of J.D. Bernal [1] and G.D. Scott [2] around 1960, the existence of a barrier to compaction has been confirmed for many types of disturbances [3–6], but not for cyclic shear for which the systems compacted via wall-induced crystallization [7]. Walls that inhibit nucleation and precision measurements of the positions of the spherical grains recently enabled Rietz *et al.* [8] to observe homogeneous crystallization in a granular material undergoing cyclic shear.

Using Newtonian overdamped dynamics, we numerically simulate purely repulsive spherical grains undergoing cyclic simple shear strain dynamics to model granular crystallization in the Rietz *et al.* experiment [8]. The simulations allow us to tune the grain interactions, gravity, and boundary conditions to understand the essential physics that gives rise to homogeneous crystallization.

Our simulations reveal the essential physical requirements needed for crystallization in driven dissipative granular materials: volume exclusion, system confinement, and small disturbances that allow grain rearrangements. In particular, gravity, friction, and energy conservation are not required to yield homogeneous crystallization. The simulations use deterministic dynamics in contrast with the probabilistic evolution equations used in classical nucleation theory [9] to model crystallization in atomic and molecular systems.

From the simulations we show that the volume fraction at the onset of crystallization becomes independent of the shear amplitude for sufficiently small amplitudes, $A \leq 0.05$ rad, consistent with Rietz *et al.* [8], who used $A = 0.01$ rad. The volume fraction at the onset of crys-

tallization is also within the range of jamming volume fractions found for different packing generation protocols for frictionless hard spheres [11].

Methods. We simulate cyclic simple shear of frictionless monodisperse spheres in three spatial dimensions using a discrete element method (see Supplemental Materials (SM), Sec. B [10]). Figure 1(a) shows the simulation shear cell, designed to mimic the parallelepiped shear cell used in experiments [7] with two sidewalls that tilt with respect to the vertical axis by a variable angle θ in the x-y plane, and a bottom wall that oscillates horizontally and can move vertically under an applied load. The system is periodic in the z-direction. The initial jammed packing is prepared via gravitational deposition by pouring the grains into a static container and allowing the dissipative forces to remove the kinetic energy in the system. A subsystem, of size $(L + 2d) \times (1.675)L \times L$ in the x-, y-, and z-directions, is cut out from the initial packing, where d is the grain diameter (see Fig.1(b)). Grains with center positions less than d away from all of the surfaces of the subsystem except the two in the z direction are then fixed to form the walls. Wall-induced crystallization is suppressed since the grains forming the walls are randomly positioned. Simulations were run for cells with edge lengths $L/d = 13$, 15, 17, and 20 containing, respectively, $N = 5200$, 7900, 11400, and 18200 grains. The selection of the simulation time step size is discussed in SM Sec. B.3 [10].

The grains are modeled as frictionless spheres interacting via the pairwise, purely repulsive linear spring force,

$$\vec{F}_{ij} = kd\delta_{ij}\Theta(\delta_{ij})\hat{r}_{ij}, \qquad (1)$$

where k is the spring constant (see SM Sec. B.1 [10]), $d\delta_{ij} = 1 - r_{ij}/d$ is the intergrain overlap, r_{ij} is the center-to-center separation between grains i and j, $\Theta(x)$ is the

Heaviside step function, and $\hat{r}_{ij}$ is the unit vector pointing from the center of grain j to the center of grain i. The interaction between the fixed wall grains and the interior grains follows the same force law as that between pairs of interior grains. Under gravity in the y-direction, Newton's equation of motion for each interior grain i is given by

$$m\vec{a}_i = \sum_{j=1}^{n_i} \vec{F}_{ij} - b(\vec{v}_i - \vec{v}_{\text{fluid}}) - m_i g\hat{y}, \qquad (2)$$

where $g\hat{y}$ is the acceleration due to gravity, m_i, $\vec{a}_i$, and $\vec{v}_i$ are the mass, acceleration, and velocity of grain i, n_i is the number of grains overlapping grain i, and b is the damping constant. The damping force arises from Stokes drag with the assumption of the existence of fluid in the cell, as in the experiment of Rietz $et\ al.$ We consider two forms for $\vec{v}_{\text{fluid}}$ for the Stokes drag; see SM Sec. B.2 [10]. We also consider The equations of motion are integrated using a modified velocity-Verlet scheme. We are interested in simulating grains in the hard sphere limit; the relationship between the spring constant and the interparticle overlap is discussed in SM Sec. B.1 [10]).

To shear the packing, the bottom wall oscillates in the x-direction (see Fig. 1 (a)) as the two sidewalls tilt with an angle θ that evolves with time t as

$$\theta(t) = A\sin(\omega t), \qquad (3)$$

where A is the shear amplitude and ω is the angular frequency. We study shear amplitudes $A = 0.03, 0.04, 0.05, 0.0667, 0.0833$, and 0.10 rad. The oscillating bottom wall consists of N_b grains and is subjected to a force $\vec{F}_{b,j}$ from interior grains. The motion of the bottom wall due to the applied pressure P can be obtained by solving

$$m_b\vec{a}_b = \sum_{j=1}^{n_b} \vec{F}_{b,j} - b(\vec{v}_b - \vec{v}_{\text{fluid}}) - m_b g\hat{y} + \frac{L^2}{N_b}P\hat{y}, \quad (4)$$

where m_b is the total mass of grains in the bottom wall and $\vec{a}_b$ and $\vec{v}_b$ are the acceleration and velocity of the bottom wall, which is constrained to move along the direction, $\hat{n} = (\sin\theta(t), \cos\theta(t), 0)$, at time t. The values of the simulation parameters are listed in Table I.

An alternative energy relaxation method was also considered, closer to that used in the experiment of Rietz $et\ al.$ [8]. Simulations with amplitude $A = 0.05$ rad were carried out with the grains allowed to come to rest after each cycle of the walls, instead of moving the walls and dissipating energy continuously. Fig. S4 in Supplemental Material Sec. B.4 shows that the results for the fraction of crystallized grains versus volume fraction ϕ using the two relaxation methods is similar until $\phi \approx 0.646$.

Results. Intuitively, the global volume fraction ϕ of a collection of grains in a container is the sum of the volumes of the grains divided by the volume of the container. If one partitions the volume of the container by

TABLE I. Parameters used in the discrete element method simulations of cyclic simple shear.

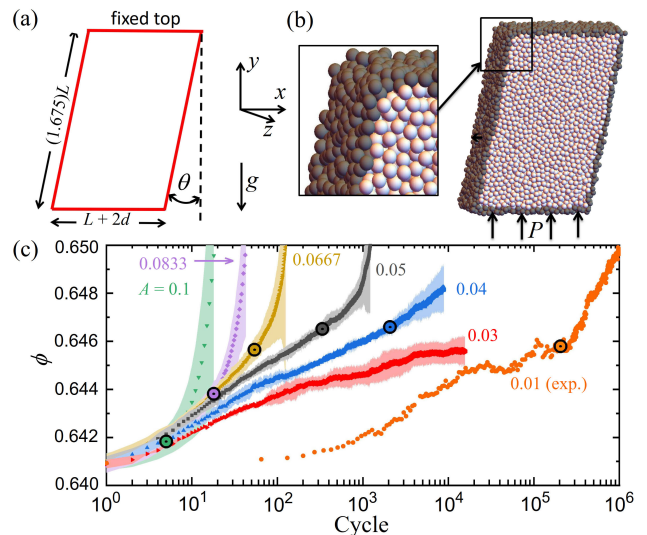| Parameter	Value
Grain mass m	2×10^{-5} kg
Grain diameter d	3×10^{-3} m
Spring constant k	6.54×10^2 N/m
Damping constant b	1.28×10^{-3} kg/s
Pressure P	9.54×10^2 Pa
Angular frequency ω	π rad/s
Simulation steps per cycle	45600
Gravitational acceleration g	9.81 m/s^2

FIG. 1. (a) Cell used for simulations of frictionless spheres undergoing cyclic shear with $\theta = A\sin(\omega t)$. The cell dimensions are $(L+2d) \times (1.675)L \times L$, where d is the diameter of the spheres; the boundary conditions in the z-direction are periodic. Simulations were conducted for L varying from $13d$ to $20d$. (b) The dark colored spheres on the cell boundary are fixed in disordered positions to inhibit crystallization. The light colored spheres in the cell interior move in the cyclically sheared cell in response to interactions with one another, the dark spheres, and gravity. A constant pressure P is applied on the bottom wall, which can move up and down. (c) The volume fraction ϕ as a function of cycle number in the simulations; the shading shows the standard deviation in simulations with different initial conditions. The results for $A = 0.01$ rad (orange points) are from the experiments by Rietz $et\ al.$ experiment [8]. The black circle with colored interior on each curve shows the value of ϕ at the onset of rapid growth of crystallites in that system.

the Voronoi cells of the grains, one has a useful local version, the local volume fraction ϕ_{local} for that Voronoi cell or grain. Our grains are slightly deformable so there is some choice in how to assign a volume to them. We are interested in modeling asymptotically hard grains, as in the experiment Rietz $et\ al$, so we define the volume of a grain to be $(\pi d^3/6)(1 - \delta_{max})^3$, where δ_{max} is the
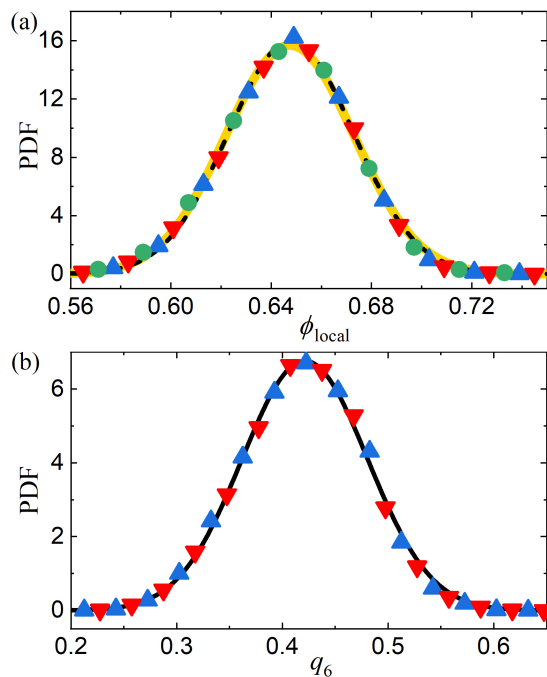
FIG. 2. (a) The probability distribution function for the local volume fraction ϕ_{local} becomes *time-invariant*, as illustrated by the simulation results for shear amplitude $A = 0.03$ rad at $n = 10000$ shear cycles (blue upward triangles, $\phi = 0.64581 \pm 0.00003$) and 15000 shear cycles (red downward triangles, $\phi = 0.64593 \pm 0.00003$). The green circles are results from the Rietz *et al.* experiment [8] with $A = 0.01$ rad, averaged over shear cycles from 18849 to 67374, where the volume fraction remained constant at 0.6449 ± 0.0001. The black and yellow curves are respectively Gaussian fits to the data for the simulations and experiment. (b) The probability distribution function for the local bond orientational order parameter q_6 is also time-invariant, as illustrated by these results at $n = 10000$ (blue upward triangles) and 15000 shear cycles (red downward triangles). The black curve is a Gaussian fit.

maximum of the 'overlap' volume of that sphere with its neighbors (see Supplemental Material Sec. B.1). The global volume fraction of a collection of grains is then the mean of the local volume fractions of all the 'free' grains, that is, the grains which are fixed as part of the boundary are not counted.

The results for the global volume fraction ϕ obtained in our simulations for shear amplitudes $A = 0.03, 0.04, 0.05, 0.068, 0.083,$ and 0.10 rad are shown in Fig. 1(c), along with results from the experiment of Rietz *et al.* [8] for $A = 0.01$ rad. The volume fraction increases in a similar way for each shear amplitude for the first few shear cycles (i.e., $n < 10$), while subsequently the increase in volume fraction is more rapid for larger shear amplitudes, as seen already by Scott experimentally [7].

At low shear amplitudes and for sufficiently small cycle numbers, the system remains disordered. Figure 2(a) shows, for $A = 0.03$ rad and several cycle numbers, prob-
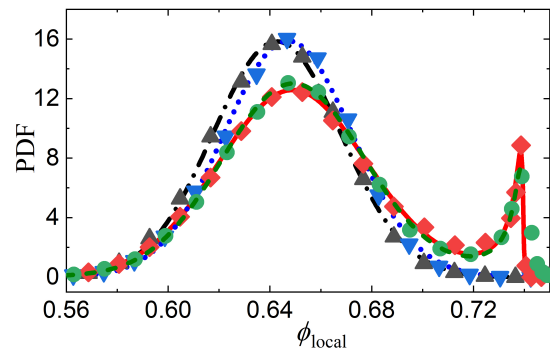

FIG. 3. Probability distribution function of the local volume fraction ϕ_{local} for $\phi = 0.6406$ (black upward triangles), 0.6450 (blue downward triangles), and 0.6538 (red diamonds), from simulations with $A = 0.05$ rad. The black and blue curves are Gaussians. For $\phi = 0.6538$ (red diamonds), the probability distribution has a second peak at $\phi_{\text{local}} \sim 0.74$, which corresponds to crystallites with FCC and HCP symmetry. Experimental data (green circles) for $A = 0.01$ rad at the same ϕ also possess a peak at $\phi_{local} \sim 0.74$. The simulation and experimental data at $\phi = 0.6538$ can be fitted as the sum of a Gaussian $g(\phi_{\text{local}})$ and an inverse Gaussian $f(\phi_{\text{local}})$ (red and green curves), $P(\phi) = ag(\phi_{local}) + (1-a)f(\phi_c - \phi_{local})$, where $\phi_c = \pi/3\sqrt{2}$ (the few data points beyond ϕ_c are not included in the fit).
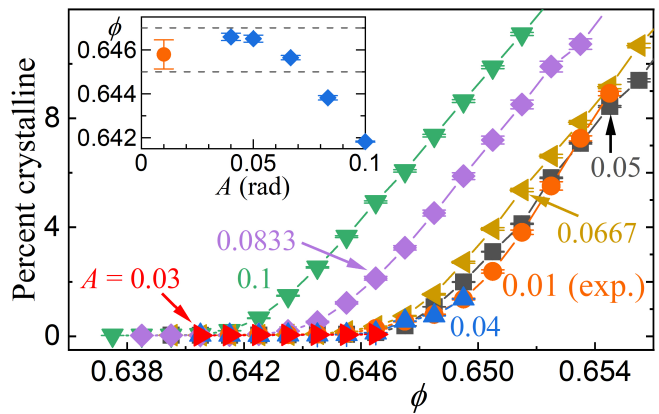

FIG. 4. The percentage of grains that are in crystallites as a function of the volume fraction is shown for simulations with $A = 0.03$ to 0.10 rad and for the experiment with $A = 0.01$ rad (orange circles) (Rietz *et al.*). The results from the simulations with $A = 0.05$ rad and the experiments with $A = 0.01$ rad are remarkably similar. The inset shows that the volume fraction at the onset of crystallization approaches a well-defined value as the shear amplitude decreases (blue diamonds: simulations; orange circle: experiments). The volume fraction at onset is defined to correspond to the emergence of a positive growth rate for the largest crystallite (10 grains for $A = 0.01, 0.04,$ and 0.05; 13 for $A = 0.0667$; 16 for $A = 0.0833$; and 20 for $A = 0.10$).

ability distribution functions for the local volume fraction ϕ_{local}. These probability distributions become time-invariant after $n \sim 10000$ shear cycles. Figure 2(b) shows time invariance also in the probability distribution functions for the local bond orientational order q_6 [12], which we use to identify crystallization; see Supplemental Material Sec. A for background. Similarly, the experiment with $A = 0.01$ rad reached a persistent state at 1.1×10^5 shear cycles (see Fig. 1(c)).

The simulations with amplitudes $A \geq 0.05$ rad do not give rise to a persistent state, as can be seen in Fig. 1(c). Further, Fig. 3 shows that for $A = 0.05$ the probability distribution function for the local density starts as a Gaussian with a peak near $\phi_{\text{local}} = 0.65$. With an increasing number of shear cycles, the height of this peak decreases and its width increases. With continued shearing, a second peak emerges at $\phi_{\text{local}} \approx 0.74$ in both the experiment with $A = 0.01$ rad and in the simulations with $A = 0.05$ rad. (Thus, the persistent state in the simulations at $A = 0.03$ rad begins to disappear for shear amplitudes in the range $0.03\,\text{rad} < A < 0.05\,\text{rad}$ and is absent for larger A.) The second peak in the probability distribution at $\phi_{\text{local}} \approx 0.74$ corresponds to the formation of HCP and FCC crystallites.

Figure 4 presents results for the fraction of the system that is crystalline in simulations with different amplitudes A. (The identification of crystalline grains is discussed in SM Sec. A [10].) The similarity between the results from the simulation for $A = 0.05$ rad and the experiment for $A = 0.01$ rad is remarkable considering the many differences between the simulation model and the laboratory experiment. For $A > 0.05$ rad (i.e., 0.067, 0.083, and 0.10 rad), the crystallization onset occurs for a smaller volume fraction than the onset observed in the experiment.

We have considered several methods for obtaining an accurate estimate for the volume fraction at the onset of crystallization in a system satisfying the limits of small shear amplitude and large system size. The method used for the inset of Fig. 4 is to determine the critical cluster size for each shear amplitude A and identify the associated value of the volume fraction; see Supplemental Material Sec. C for a comparison with an alternative method for determining the volume fraction at the onset of crystallization. Both methods are in quantitative agreement, yielding the results in the inset of Fig. 4.

Discussion. The results obtained from the simulations of the deterministic equations of motion for frictionless monodisperse spheres in a container undergoing periodic shear reveal the onset of homogeneous crystallization that depends on the shear amplitude A and on the number of grains N in the system. However, the simulations show that there is a well-defined volume fraction, $\phi = 0.646 \pm 0.001$, above which homogeneous crystallization occurs in the limit of small amplitude, $A \leq 0.05$ rad (see inset of Fig. 4(a)) and large system size, $N \geq 18200$.

This characteristic volume fraction $\phi = 0.646$ agrees well with the experimental value found in Rietz *et al.* [8], where $A = 0.01$ rad and $N = 49400$.

Note that there are multiple differences between the experiment by Rietz *et al.* and the simulations, including the form of the dissipation, which in the experiment arises from Stokes drag on the motion of the grains relative to the viscous refractive-index-matching fluid surrounding the grains, from the inelasticity of the grains, and from the static and dynamic friction between grains in contact. In contrast, in the simulations only Stokes dissipation is included; the static and kinetic friction coefficients are zero. Still, the results for the onset of crystallization in the simulations and the Rietz *et al.* experiment agree in the limits of hard-sphere interactions, low driving amplitude, and large system size.

The *random close packed* (RCP) limit, which has been discussed in more than one thousand papers in the past half century, has never been unambiguously defined and may well be different for different physical compaction protocols [13]. However, for cyclic simple shear (in the quasistatic limit), we find a well-defined value of the global volume fraction, 0.646 ± 0.001 at the onset of crystallization. This value, which is in the reported range for RCP, 0.62-0.66, is robust to friction, gravity, and amplitude changes in the small amplitude limit. To avoid confusion we refer to the value we obtain as the 'crystallization volume fraction for asymptotically small shear amplitudes.'

There are compaction protocols, such as cyclic shear coupled with horizontal and vertical shaking, for which the particles or grains possess significant kinetic energy that is slowly drained during the compaction process. For such protocols, it is possible as noted above, that the volume fraction for the onset of crystallization may occur at a different value than the one found here. One method to investigate this question is to carry out simulations of cyclic shear for underdamped, frictionless grains with weak damping, in addition to weak horizontal vibrations. Then the onset of crystallization could be determined as a function of the damping coefficient [14] as well as in the limit of small shear and vibration amplitudes.

Physical nongranular crystallization experiments and their modeling, in particular the homogeneous freezing of molecular fluids [9], should be compared with the homogeneous crystallization in the present simulations and in Rietz *et al.* [8] and [15]. In particular, persistent states play an important role in classical nucleation theory but seem to play a marginal role in these simulations and experiment, disappearing with growing shear amplitude.

*microwei.jin@gmail.com **shattuck@ccny.cuny.edu

———————

[1] J.D. Bernal, A geometrical approach to the structure of liquids, Nature (London) **183**, 141 (1959).

[2] G.D. Scott, Packing of equal spheres, Nature (London) **188**, 908 (1960) .

[3] J. B. Knight, C. G. Fandrich, C. N. Lau, H. M. Jaeger, and S. R. Nagel, Density relaxation in a vibrated granular material, Phys. Rev. E **51**, 3957 (1995); P. Richard, M. Nicodemi, R. Delannay, P. Ribiere, and D. Bideau, Slow relaxation and compaction of granular systems, Nat. Mater. **4**, 121 (2005).

[4] S. R. Liber, S. Borohovich, A. V. Butenko, A. B. Schofield, and E. Sloutskin, Dense colloidal fluids form denser amorphous sediments, PNAS **110**, 5769 (2013).

[5] K. Chen, J. Cole, C. Conger, J. Draskovic, M. Lohr, K. Klein, T. Scheidemantel, and P. Schiffer, Packing grains by thermal cycling, Nature (London) **442**, 257 (2006).

[6] M. Schröter, D. I. Goldman, and H. L. Swinney, Stationary state volume fluctuations in a granular medium, Phys. Rev. E **71**, 030301 (2005).

[7] G.D. Scott, A.M. Charlesworth, and M.K. Mak, On the random packing of spheres, J. Chem. Phys. **40**, 611 (1964); M. Nicolas, P. Duru and O. Pouliquen, Compaction of a granular material under cyclic shear, Eur. Phys. J. E **3**, 309 (2000).

[8] F. Rietz, C. Radin, H. Swinney and M. Schröter, Nucleation in sheared granular matter, Phys. Rev. Lett. **120**, 055701 (2018).

[9] F. F. Abraham, *Homogeneous Nucleation Theory* (Academic Press, New York, 1974); P. Debenedetti, *Metastable Liquids* (Princeton University Press, Princeton, NJ, 1996).

[10] See the Supplemental Material at http://link.aps.org/supplemental/XX/PhysRevLett.XX for discussions of the identification of the crystalline grains (Sec. A); the computational method, including the dependence on the spring constant magnitude (Sec. B.1), drag force (Sec. B.2), simulation timestep size (Sec. B.3), and the protocol used for energy relaxation (Sec. B.4); the determination of the critical cluster size (Sec. C); the role of gravity (Sec. D); and the homogeneity of the nucleation process (Sec. E).

[11] P. Chaudhuri, L. Berthier, and S. Sastry, Jamming transitions in amorphous packings of frictionless spheres occur over a continuous range of volume fractions, Phys. Rev. Lett. **104**, 165701 (2010).

[12] P. J. Steinhardt, D.R. Nelson, and M. Ronchetti, Bond-orientation order in liquids and crystals. Phys. Rev. B **28**, 784 (1983).

[13] S. Torquato, T. M. Truskett, and P. G. Debenedetti, Is random close packing of spheres well defined?, Phys. Rev. Lett. **84** 2064 (2000); C. Radin, Random close packing of granular matter, J. Stat. Phys. **131** 567 (2008); Y. Jin and H. A. Makse, A first-order phase transition defines the Random close packing of hard spheres, Physica A **389** 5362 (2010).

[14] S. S. Ashwin, J. Blawzdziewicz, C. S. O'Hern, and M. D. Shattuck, Calculations of the basin volumes for mechanically stable packings, Phys. Rev. E **85**, 061307 (2012).

[15] C. Radin and H. L. Swinney, Phases of granular matter, J. Stat. Phys. **175**, 542 (2019).